

CHANDRA POCKET GUIDE

Chandra Instruments

Instrument	FOV (arcmin)	Pixel (size/arcsec)	Energy Resolution (ev at 1 keV)	Timing Resolution (s)	On Axis Effective Area (cm ² at 1 keV)
ACIS-I	16.9 × 16.9	0.492	60 [◇]	3.2 [*]	367 (FI)
ACIS-S	8.3 × 50.6	0.492	120 (BI), 60 (FI)	3.2 [*]	367 (FI), 555(BI)
HRC-I	30 × 30	0.13	~1000	16 × 10 ⁻⁶	227
HRC-S	6 × 99	0.13	~1000	16 × 10 ⁻⁶	227

[◇] Energy resolution of FI chips are row-dependent

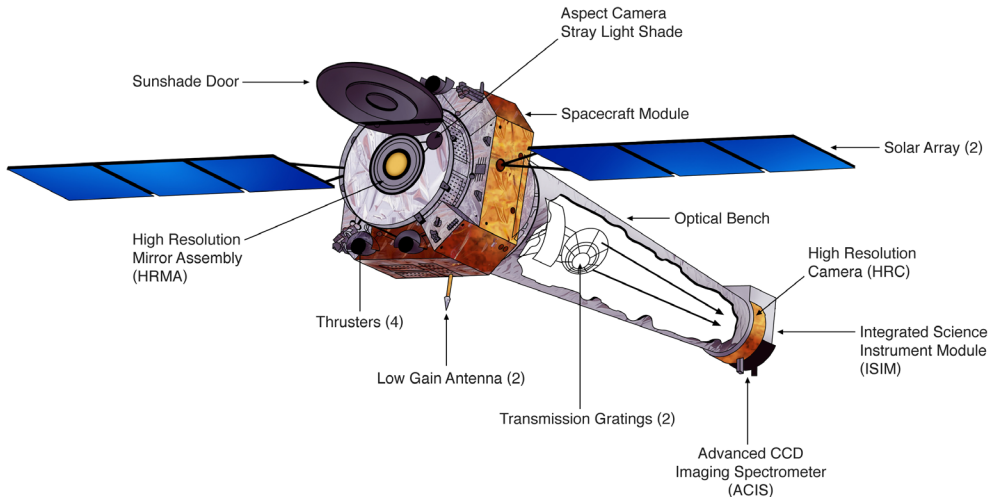
^{*} Number for full frame, <3.2s for subarray, down to 0.8s for 1/4 subarray

Chandra Spectrometers

Spectrometer	Wavelength Range	Resolving Power ($E/\Delta E$)		Effective Area (cm ²)	
		1 keV (12.4Å)	6.4 keV (1.9Å)	1 keV (12.4Å)	6.4 keV (1.9Å)
HETG+ACIS-S	0.4–10.0 keV (1.2–31Å)	1000	150	59	28
LETG+ACIS-S	0.2–10.0 keV (1.2–60Å)	250	40	23	20
LETG+HRC-S	0.07–10.0 keV (1.2–175Å)	250	40	24	4

HETG effective areas include HEG plus MEG first orders summed

LETG effective areas include first orders, positive and negative, summed



Contents

- 5 High-Resolution Mirror Assembly (HRMA)
- 6 Advanced CCD Imaging Spectrometer (ACIS)
- 11 High-Resolution Camera (HRC)
- 12 Gratings
- 15 Pointing Control & Aspect Determination (PCAD)
- 16 Proposals
- 20 CIAO and Obtaining Datasets
- 21 Ray Tracing/Simulations

About Chandra

The *Chandra X-ray Observatory* is one of NASA's "Great Observatories" and was launched on July 23, 1999 aboard the Space Shuttle *Columbia*. It is one of the largest satellites ever launched by the Space Shuttles. *Chandra's* primary purpose is to detect X-ray emission from extremely hot regions of the Universe, such as exploded stars, galaxy clusters, and the material surrounding black holes. Because X-rays are absorbed by Earth's atmosphere, *Chandra* is in Earth orbit. The orbit is highly elliptical; as of 2023, the orbital period is 63 hours and 28 minutes. *Chandra's* orbit extends up to an altitude of 147,400 km in space and takes the spacecraft more than $\frac{1}{3}$ of the way to the Moon.

Chandra's High-Resolution Mirror Assembly (HRMA) is a 10-meter focal length telescope consisting of two sets of four nested cylindrical, grazing-incidence, glass-ceramic mirrors coated with iridium to enhance their reflectivity at X-ray wavelengths. This technology is what has allowed *Chandra* to achieve its remarkable advance in angular resolution, with a sub-arcsecond full width at half maximum.

The *Chandra X-ray Center* (CXC), located in Massachusetts and managed by the Smithsonian Astrophysical Observatory (SAO) for NASA, is responsible for all aspects of the *Chandra* mission, including data processing and distribution to scientists worldwide for analysis.

About This Document

The *Chandra* Pocket Guide is designed to be a quick overview and reference for new users in the scientific community. For a more thorough discussion of *Chandra*, its instruments, and capabilities, please refer to the Proposers' Observatory Guide (POG, cxc.harvard.edu/proposer/POG/). The POG is updated annually.

For further information about data analysis, visit the CIAO website (cxc.harvard.edu/ciao/).

High-Resolution Mirror Assembly (HRMA)

The *Chandra* X-ray telescope consists of four pairs of concentric thin-walled, grazing-incidence Wolter Type-I mirrors called the HRMA. The front mirror of each pair is a paraboloid and the back a hyperboloid. The eight mirrors were fabricated from Zerodur® —a glass-ceramic that is highly resistant to thermal expansion at extremely cold temperatures—figured, polished, and coated with iridium on a binding layer of chromium.

The largest mirror has a diameter of 1.2 m and the focal length is 10 m. HRMA has an angular resolution of better than 0.5 arcsec (FWHM); 12 times better than *XMM-Newton*, 50 times better than *ROSAT*, and able to resolve the cosmic X-ray background.

While the unobscured geometric aperture of the HRMA is 1145 cm², the effective area depends on X-ray photon energy and grazing angle. Each additional nested mirror layer contributes to the effective collecting area. The inner layers have more sensitivity to harder photons and the outer layers have more sensitivity to softer photons.

During fabrication, scientists and engineers polished and ground the four pairs of mirrors to the smoothness of a few atoms. At the time, they were the smoothest mirrors ever made.

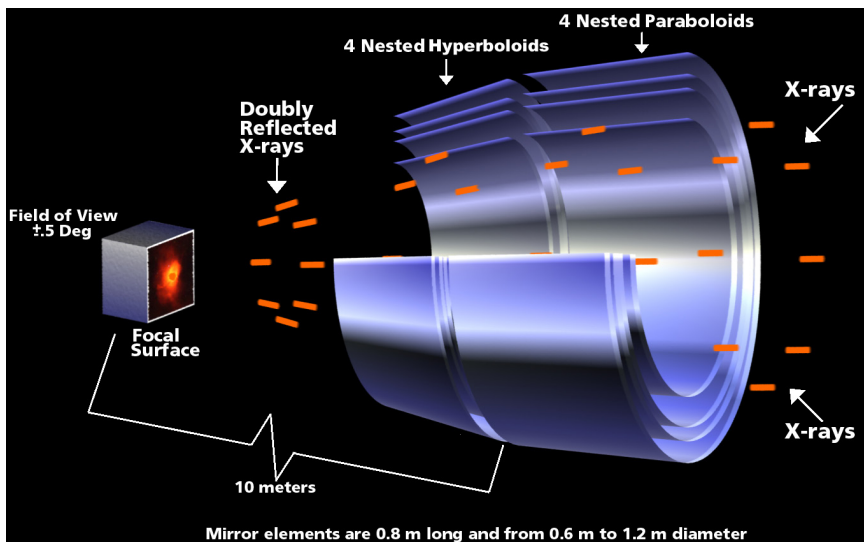


Illustration of Chandra's HRMA mirrors. X-rays that strike a mirror head-on are absorbed. X-rays that hit a mirror at grazing angles are reflected like a pebble skipping across a pond. Thus, X-ray telescope mirrors are shaped like barrels rather than dishes.

Advanced CCD Imaging Spectrometer (ACIS)

ACIS has 10 chips (shown to the right); four arranged in a 2×2 array (ACIS-I), and six arranged in a 1×6 array (ACIS-S) with a single CCD having an $8.3' \times 8.3'$ field-of-view (FOV). There are two naming conventions for the ACIS CCDs, either by array or number: I0–I3 and S0–S5 or enumerated 0–3 and 4–9, respectively. The energy range for ACIS is 0.2–10 keV. ACIS-I provides optimal imaging over its large FOV while ACIS-S is used for imaging or grating spectrum read-out. While the nominal ACIS channel bin width is 14.6 eV, the detector linespread yields spectral resolution of 95 eV (at 1.49 keV) and 150 eV (at 5.9 keV) at the back-illuminated (BI) S3 chip aimpoint. At the front-illuminated (FI) I3 chip aimpoint, the spectral resolution is 130 eV (at 1.49 keV) and 280 eV (at 4.9 keV). Early in the mission, the BI chips had better sensitivity to soft pho-

Standard Read-out Mode

Timed Exposure

Events are integrated over a preselected amount of time—a.k.a. the “*Frame Time*.” The default frame time is about 3 seconds. Once this time interval has passed, the charge from the active region of the detector is read out. This takes an additional 41 μs .

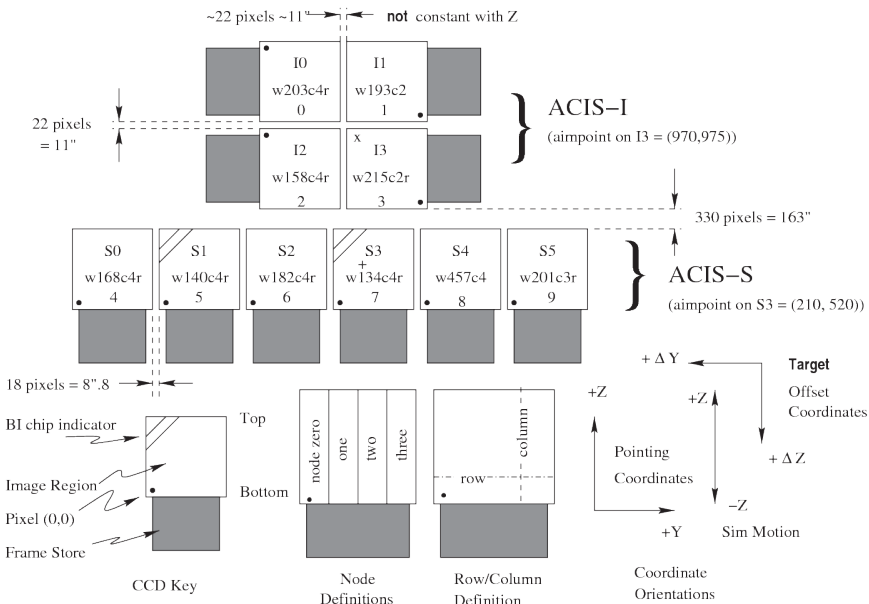
Non-Standard Read-out Modes

Alternating Exposure (a.k.a. Interleaved)

Read-out exposures alternate between a long frame time and a short frame time. This mode can, for example, be used to observe data on a diffuse source with embedded bright point sources with a single pointing so that the observer gets the piled long-frame information useful for the diffuse source, as well as the unpiled short-frame data for the point sources.

Continuous Clocking (CC)

Uninterrupted data read-out resulting in an effective integrated frame time of 2.85 ms. The high time resolution comes with the loss of one spatial dimension.



ACIS focal plane. Note the positions of the back-illuminated S3 chip aimpoint and the front-illuminated I3 chip aimpoint.

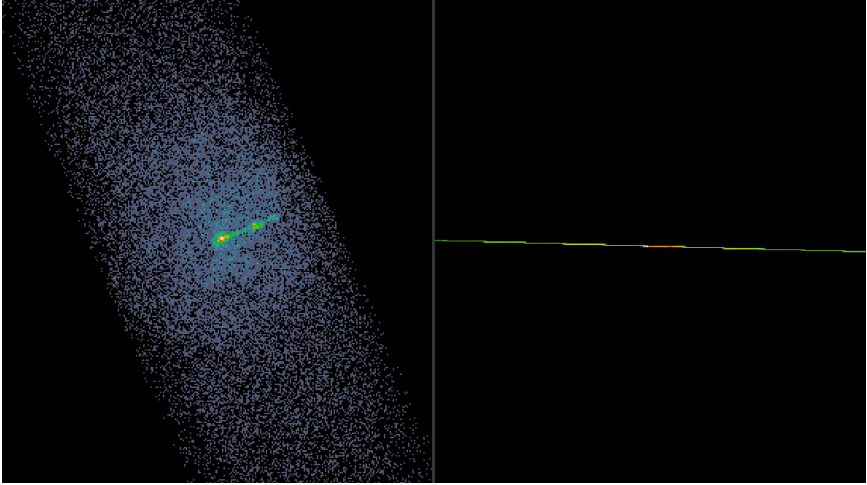
tons over the FI chips; however with the build up of contaminants on the detector, the difference has diminished.

X-ray photons hitting the camera are detected individually and their position, energy, and arrival time recorded, allowing for the simultaneous creation of images, spectroscopy, and light curves. In the past, up to six CCDs could be active throughout an observation. But since Cycle 21, due to stricter thermal constraints, a maximum of four CCDs may be specified as required for an observation while a fifth and/or sixth may be selected as optional and will be dropped if necessary.

When ACIS-S is used with the High-Energy Transmission Grating (HETG) it provides up to 1000 resolving power ($E/\Delta E$) from 1.2-10.0 keV. This combination has been used to measure Doppler velocities as low as 50 km/s, and plasma outflow velocities from a few hundred to tens of thousands of km/s. Because the HETG can clearly resolve lines from O to Fe-K, detailed line diagnostics can be applied.

When observing very bright or fast changing sources, both ACIS-S and ACIS-I can also be used in continuous clocking mode, which allows for continuous chip read-out at 2.85 ms per row, but

loses one spatial dimension. Because all the events are collapsed onto a single spatial axis in CC-mode, only one spatial coordinate per event is available.



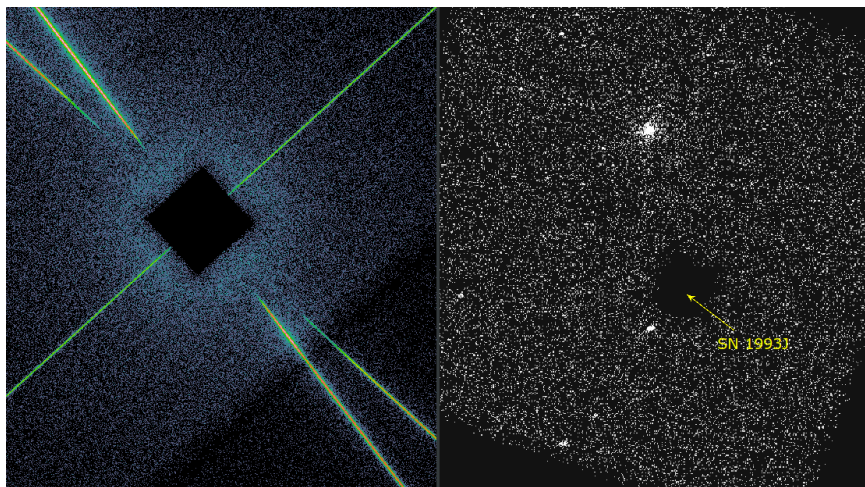
ACIS-S observations of M87. The observation on the right was captured in CC-mode, eliminating one spatial dimension.

In TE-mode, it's possible to adjust the frame time and use sub-arrays. Frame times are selectable within a range of values spanning the time interval of 0.2 to 10.0 s. If the data from the entire CCD are utilized (full frame) then the nominal (and optimal) frame time is between 3.0 to 3.2 s, as a function of the number of active CCDs (up to six). Selecting a frame time shorter than the nominal value has the consequence that there will be a time during which no data are taken, “deadtime”, since this nominal amount of time is required for the full frame store read-out process, regardless of the frame time. The below equation calculates the fraction of time during which data are taken, where t is the selected frame time, T_{opt} is the optimal frame time, and 0.041 is the framestore transfer time in seconds.

$$t / (T_{opt} + 0.041)$$

For example, an observation that uses the full 1024×1024 frame of a single CCD has a nominal frame time of 3.0 s. Therefore, if the user instead picks a frame time of 0.2 s, a 30 ks long observation would have less than 2 ks of effective exposure time.

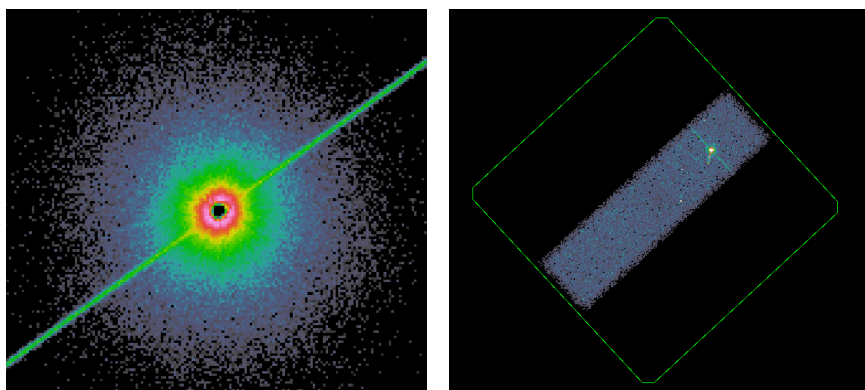
Sub-arrays are a subset of the available pixel rows on the active CCDs that the observer may select to be used for an exposure resulting in a short nominal frame time, as low as 0.3 s. The low frame time reduces observed pile-up while minimizing the deadtime, which preserves high observing efficiency in the smaller FOV.



Spatial windows. Left: ACIS-S/HETG observation of Cyg X-2. Right: ACIS-S observation of M81.

(Pile-up occurs whenever two or more photons are detected as a single event and represents a loss of information from these events. This also distorts the energy spectrum.)

The telemetered data mode format also determines the data bit size per event. The number of bits per event, in turn, determines the event rate at which the telemetry will saturate and data will be lost until the on-board buffer empties. Bright sources are susceptible to telemetry saturation and unfortunately, this means that full frame exposures are dropped, resulting in reduced effective observing time. Dropped ACIS frames can be avoided by onboard event



Left: ACIS-S/HETG observation of GRS 1915+105. Notice the dark pileup region in the middle and the readout streak extending to both sides of the object. Right: Subarrayed ACIS-S observation of quasar 4C 19.44. The proposal requested a specific roll to keep the readout streak away from the jet. The green box represents the full FOV of the CCD.

filtering with Graded data mode or applying a spatial window to the read-out data to limit/exclude events in specified portions of the detector from the downlinked telemetry stream.

Since the ACIS detector does not have a shutter, some events are detected during the period taken to transfer the exposed frame to the framestore to be read out. These events are detected with the CCD column they fall on but are readout with incorrect rows, randomly spread all along their columns. For a bright source, a uniform streak is generated in the readout direction (on both sides of the source, since some events are from the previous exposure), and this effect is interchangeably referred to as: ‘read-out streak’, ‘trailed image’,

Telemetered Data Formats

Faint

The faint format provides event position in detector coordinates, an arrival time, an event amplitude, and the amplitude of the signal in each pixel in the 3×3 event island that determines the event grade.

Very Faint (VFaint)

The very faint format provides event position in detector coordinates, the event amplitude, an arrival time, and the pixel values in a 5×5 island. This format is only available with TE-mode and events are graded by the contents of the central 3×3 island. The very faint mode offers the advantage of reduced background rates after ground processing, but only for sources with low counting rates that avoid both telemetry saturation and pile-up.

Graded

The graded format provides event position in detector coordinates, an event amplitude, the arrival time, and the event grade. Note that certain grades may not be included in the data stream. Event grading and rejection are performed on-board at the expense of not preserving a full set of event properties. This mode is typically used for very bright sources that would be prone to telemetry saturation.

‘read-out artifact’, ‘transfer smear’, or ‘out-of-time events’. These out-of-time events contribute to the observed background which can be especially important when analyzing bright, extended emission, and a generalization to note is that a source bright enough to have a read-out streak will have some degree of pile-up. The artifact can interfere with spatial analysis. However, for extremely bright sources there are sufficient number of events that the read-out streak can be taken advantage of to extract an unpiled spectrum or perform timing analysis with 40 μs resolution.

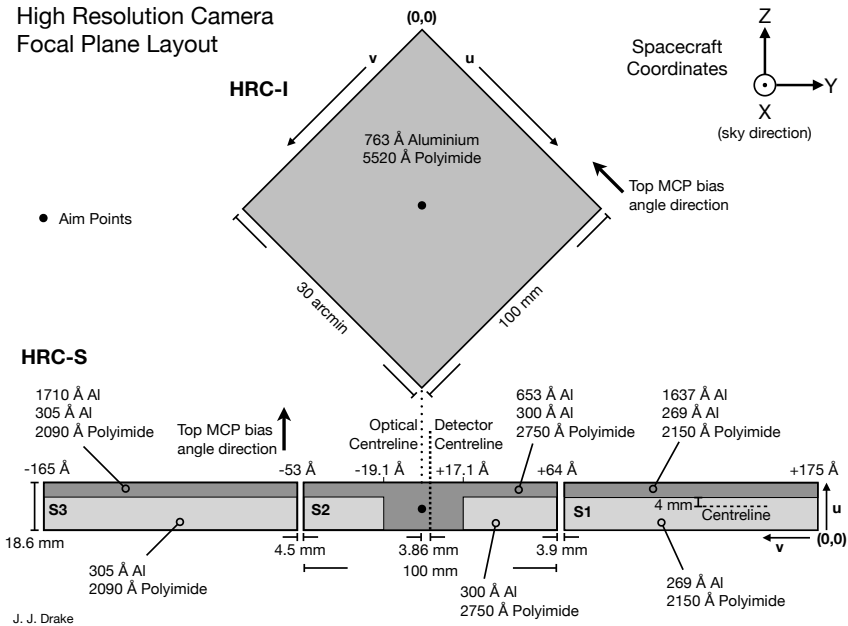
High-Resolution Camera (HRC)

The HRC is a microchannel plate instrument with two detectors and provides the highest on-axis spatial resolution. The HRC energy range (0.06–10 keV) extends below that of ACIS. HRC-I is intended for imaging and provides the largest FOV aboard *Chandra*; HRC-S is intended for spectroscopy. Given the nature of microchannel plates, there is no energy discrimination for the events, so HRC has negligible spectral resolution without the use of gratings. There are techniques to differentiate between hard and soft events, but only approximate hardness ratios can be provided.

When used with the Low-Energy Transmission Grating (LETG), HRC-S provides the highest spectral resolution (up to 2000) on *Chandra* at low energies (0.08–0.2 keV). This combination is used for high resolution spectroscopy of soft sources such as stellar coronae, white dwarf atmospheres, and cataclysmic variables. HRC-S can also be used in a very fast timing mode, which provides a maximum time resolution of 16 μs .

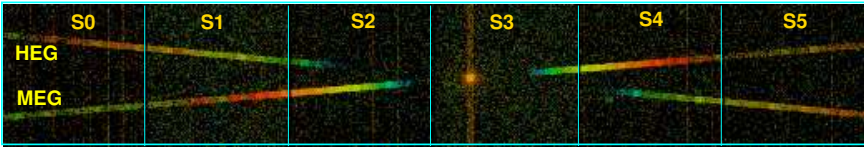
While the HRC detectors were designed to have a 16 μs time resolution, a wiring error causes event timing accuracy to be degraded to an uncertainty of roughly on the order of $1/\dot{C}$ for any given event count where \dot{C} is the total observed count rate. The “HRC timing” science instrument mode was subsequently developed to recover the intended time resolution by using only a very small portion on the central microchannel plate of the HRC-S detector. The timing accuracy is dependent on the total count rate—including the background count rate and not just the source count rate. By limiting the use of a small area near the optical-axis, the field integrated background count tends to be very low so that the total count rate is assumed to be completely dominated by non-background source events.

High Resolution Camera Focal Plane Layout



Gratings

Diffraction gratings disperse light into multiple orders, described analytically by the one-dimensional diffraction equation, $m\lambda = d \sin \theta_{\text{diff}}$, where m is the diffraction order, d is the diffraction period, λ is the event wavelength, and θ_{diff} is the diffraction angle. At any diffraction angle, different wavelengths overlap. CCD energy resolution is enough to separate orders, and hence, determine the wavelength and order for each photon (TG_M and TG_LAM in the event file) using the dispersed coordinate (TG_MLAM) and knowledge of the CCD spatial resolution and photon's CCD low-resolution energy. Grating event order sorting is done by taking the ratio of the diffraction coordinate, uniquely determined from the diffraction angle (with diffraction period stored in the CalDB $GEOM$ file), to the CCD "wavelength" as determined by the event. If the value is within the CCD resolution of an integer value, then that integer value is assigned as the order. Since the HRC detectors have little energy resolution, overlapping orders cannot be sorted. The TG_M column is either -1 or +1, and $TG_LAM = |TG_MLAM|$, to preserve consistency in format with the HETG event file.



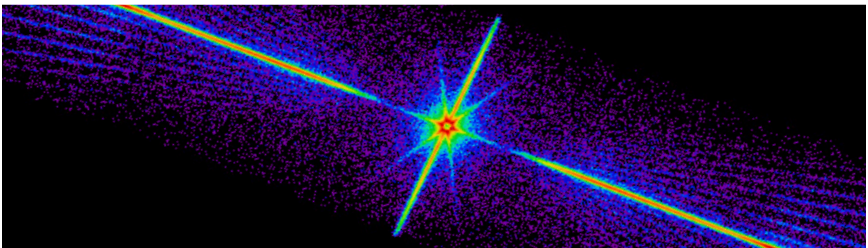
Raw ACIS-S/HETG image of Capella, color-coded by energy. The dispersed spectrum forms a shallow X on the ACIS-S array centered at the zeroth order position

High-Energy Transmission Grating (HETG)

The HETG is composed of the High-Energy Grating (HEG, 0.8–10.0 keV, 15–1.2 Å) and the Medium-Energy Grating (MEG, 0.4–5.0 keV, 31–2.5 Å) arms, the dispersed photons result in an X-shaped pattern on the detector-plane and the zeroth-order un-dispersed events may be treated as regular imaging data with the exception that its observed with reduced effective area. The background level of dispersed events tends to be very low, particularly when used in conjunction with ACIS.

Low-Energy Transmission Grating (LETG):

The LETG is optimized for high-resolution spectroscopy over the energy bandwidth ~ 0.09 –4 keV (3.1–138 Å) with a resolving power ~ 1000 at 0.1 keV and ~ 200 at 1.5 keV. The large dispersion in energy range of the LETG requires a detector that is physically large in the dispersion direction. The HRC-S is the only detector aboard that can fully accommodate the LETG-dispersed spectrum. LETG can also be used with ACIS but will have a lower quantum efficiency below ~ 0.6 keV and the higher dispersed orders will fall beyond the chip edges.



ACIS-S/LETG image of a Sun-like star orbiting a black hole. The spokes around the center are artifacts from the LETG support structure.

<i>Columns (Gratings Event File)</i>	<i>Description</i>
TG_SRCID	Source identifier index. Up to ten sources can be resolved simultaneously. The pipeline only detects the brightest source.
TG_PART	The spatial part of the spectrum: 0 - zeroth-order; 1 - HEG; 2 - MEG; 3 - LEG.
TG_R	Angular diffraction coordinate. The diffraction angle in degrees from the zeroth-order centroid, in the direction parallel to the dispersion.
TG_D	Angular diffraction coordinate. The cross-dispersion angle, in degrees. Note that the grating plate scale is slightly different from that of imaging-mode. Grating mode will maintain square pixels in (tg_r, tg_d) angular coordinates, but will not be the same as sky (x,y) angles, by a factor of about $8637/10062 = 0.858$
TG_M	If the detector has sufficient energy resolution (e.g., is ACIS), then the order can be resolved using the photon ENERGY coordinate (linearized, scaled PHA). This is the integer-valued diffraction order. TG_M may be negative. Unresolved photons are assigned a value of Null and sortable background events as 99.
TG_LAM	If the photon is resolved, then this is the wavelength, in Angstroms. TG_LAM is non-negative; unresolved photons are assigned wavelengths of 0.0.
TG_MLAM	The order multiplied by wavelength, in Angstroms.
TG_SMAP	This is a bitmap used to record whether a photon's source is ambiguous. If there are multiple sources in the field, then HETG orders will cross. It is possible that the CCD ENERGY will not resolve the photon uniquely. If not, a bit is set for each possible source. Note that only one diffraction coordinate is stored. The software cannot tell which source this photon came from.

Pointing Control & Aspect Determination (PCAD)

Chandra's Pointing Control and Aspect Determination System (PCAD) serves two primary purposes: on-board spacecraft pointing control and aspect determination, and post-facto ground aspect determination, used in X-ray image reconstruction and celestial location.

Key elements of the PCAD include the Aspect Camera Assembly (ACA), Inertial Reference Units (IRUs), and the Reaction Wheel Assembly (RWA).

The ACA is an 11.2 cm optical telescope with redundant CCDs mounted to the side of the HRMA. ACA electronics track a small pixel region around guide stars and fiducial lights. Centroids and magnitudes are calculated and used on-board by the PCAD, and are also telemetered to the ground along with the raw pixel data.

Two IRUs, each with two gyros, sense slight changes in the spacecraft's attitude and produce an electrical pulse. Beginning with a known pointing direction and adding up the electrical pulses tells the satellite's computers where it is pointed.

Control of the spacecraft momentum is required both for maneuvers and to maintain stable attitude during science observations. Momentum control is primarily accomplished by the six momentum wheels of the RWA.

In the normal science pointing mode, the PCAD system uses sensor data from the ACA and IRUs, and control torques from the RWA, to keep the target attitude within ~ 30 arcsec of the telescope boresight. This is done by optimally combining ACA star centroids (typically 5) and angular displacement data from two 2-axis gyroscopes. On short time scales ($\sim s$) the spacecraft motion solution is dominated by the gyroscope data, while on longer timescales, it is the star centroids that determine the solution. Post-facto aspect determination is done on the ground and uses more sophisticated processing and better calibration data to produce a more accurate aspect solution.

In 2018, a glitch developed in one of the gyros (IRU-2, Gyro-2). Since then, a "mixed-configuration" with one gyro from each IRU has been used. But running two different IRUs increases the heat generated by *Chandra*.

This extra heat, combined with *Chandra*'s thermal insulation degradation, makes keeping the telescope cool even more complicated. A cool ACA CCD is necessary to observe guide stars, but the increased temperature makes locking onto faint stars more difficult.

Pointing accuracy has decreased with time due to higher temperatures. As of 2022, the absolute accuracy on the pointing is 0.8 arcsec while earlier in the mission the pointing accuracy was 0.6 arcsec.

Proposals

Ever since Cycle 21 all *Chandra* proposals are submitted through the web-based *Chandra* Proposal Software (CPS, cxc.harvard.edu/proposer/CPS.html). Although most observations occur during the calendar year corresponding to the Cycle, it can take up to two years to fully complete an observing cycle, with a roughly one year overlap between cycles. While proposers may request that an observation be uninterrupted (i.e., not split into smaller segments), the maximum duration depends on the spacecraft pitch angle and the observing instrument, with significantly longer maximum dwell times possible for HRC observations as compared with ACIS at certain pitch angles. Depending on observing conditions, the maximum allowed dwell time could be as low as 10–20 ks for Cycle 25 and beyond.

It is important that anyone planning on proposing for observing time read Chapter 3 of the Proposers' Observatory Guide (POG) and the annual Call for Proposals (CfP). If you have an accepted proposal, familiarity with Chapter 2.7 of the POG provides a broad overview of the scheduling process for your observing program.

A predetermined amount of observing time each cycle is reserved for Director's Discretionary Time (DDT) which is made available to observers. This time is typically reserved for transient science such as supernovae, gamma-ray bursts/tidal disruption events, or gravitational waves, but can also provide non-transient data to benefit student research or complete a survey. Proposers must demonstrate why the science return from the proposed observation is important and cannot be submitted for peer review during the next cycle. Proposers should also note that TOO programs approved by the peer

Proposal Types

General Observing Projects (GO)

Chandra observations, generally (but not limited to) requesting less than 400 ks of observing time.

Large and Very Large Projects (LPs and VLPs)

Chandra observations requiring 400–1000 ks (LP) or >1 Ms (VLP) of observing time and designated as LP/VLP by the PI. There are no other limits to the requested exposure time of an LP/VLP or to the number of targets. During peer review, these proposals are evaluated by two separate topical panels and a big projects panel.

Target of Opportunity (TOO)

Projects that are triggered by the occurrence of an anticipated transient astrophysical phenomenon (e.g., a supernova or gravitational wave event).

Joint Observing Projects

Subclass of the above three project types that require multi-wavelength data taken by *Chandra* and one or more other facilities.

Archival Research Projects

Projects that use data from the *Chandra* archives, or the *Chandra* Source Catalog. Projects propose for funding.

Theory/Modeling Projects

Projects that seek to better understand and interpret the data that have been taken with *Chandra*, or that seek to determine what new observations might be taken to test a hypothesis. Projects propose for funding.

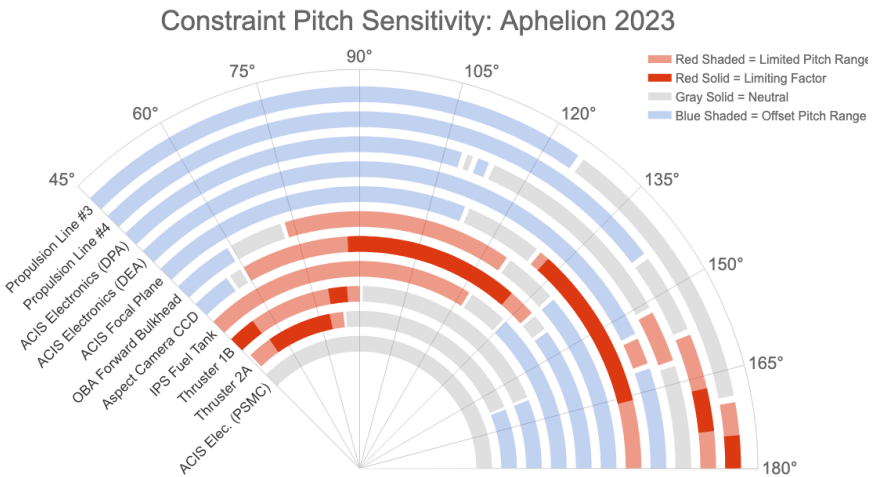
Multi-Cycle Observing Programs (MCOP)

These are a subclass of proposals for time-constrained observations that span up to two cycles into the future. All targets must be proposed for the current cycle, and proposals must justify the allocation of time across multiple cycles.

review take priority over DDT requests if the object in question fulfills the trigger criteria of a pre-approved program and proposals previously rejected by the peer review will not generally be considered for DDT.

Prior to Cycle 24, the standard proprietary period for GO programs was 12 months, which has since been reduced to six months of exclusive use, counting down from when the data are made available to the observer. For segmented observations, the six month period for each target begins when 90% of the data have been made available to the observer. For a series of discrete observations (e.g., monitoring sequences, grids) the exclusive period is established separately for each of the observations. Data from TOO and DDT programs may be exclusive for limited periods, no more than three months, before they are made publicly available. Finally, observations approved in the VLP category do not have any exclusive use period and LPs have six months of proprietary time unless a shorter time is requested by the PI.

For each observation, a resource cost (RC) and High-Ecliptic Latitude (HEL) measured in ks is calculated. The observer must be conscious of the RC and HEL budgets—see sections 4.3 and 4.5 of the CfP, respectively—as limits on these costs are expected to become stricter. Section 1.3.2 of the CfP summarizes the anticipated time allocation budget for the Cycle.



This “protractor plot” shows the thermal impact of solar pitch angle on various spacecraft components and illustrates the complicated task of keeping all components at a nominal temperature.

Some helpful points about the RC/HEL limitations to keep in mind are:

- Degradation of the thermal insulation of the spacecraft has negatively affected temperature-sensitive components. Different components undergo heating at different solar pitch angles and balancing the temperature of these components involves a significant scheduling effort. The RC has been used since Cycle 22 to quantify the difficulty of scheduling each non-TOO observation. All targets have a minimum non-zero RC derived from both the position on the sky and any user-imposed science constraints and proportional to the exposure time.
- Targets at high ecliptic latitude ($>|55|$ degrees) heat the ACA and are always at a thermally unfavorable pitch angle, which requires limiting the available time observable at these latitudes to construct a thermally balanced Long-Term Schedule. Therefore, observations of high ecliptic latitude targets are assigned a higher RC than an equivalent target at lower latitude.
- If your observations require constraints, select the necessary constraint flags in CPS. Constraints only mentioned in the proposal's scientific justification are not guaranteed to be met, resulting in data unusable to perform the proposed science.
- There are caps on the total RC and HEL time that will be accepted at the peer review and the RC for all targets within a proposal are calculated within CPS. An online RC calculator (*exc. harvard.edu/toolkit/rccalc.jsp*) for a target is also available for proposal planning purposes.

CIAO and Obtaining Datasets

The standard software package for reducing and processing *Chandra* datasets is CIAO (*Chandra* Interactive Analysis of Observations). The software is distributed as binaries and as Conda packages for Linux and MacOS systems (n.b. Windows Subsystem for Linux is not supported). CIAO contains a suite of *Chandra*-specific tools and although tailored to specialize in X-ray data analysis—to handle N -dimensional datasets—most of the tools are mission-independent and may be used to analyze non-*Chandra* datasets.

The *Chandra* Data Archive (CDA) contains all the data obtained by the telescope and there are several options to obtain the datasets. The primary gateway is ChaSeR (*Chandra* Search and Retrieval, cda.harvard.edu/chaser/), a web-based interface to the Archive allowing users to browse the observation catalog with a variety of search criteria, display preview images, and to retrieve datasets of interest as tar files, including lower level data products and engineering observations. Observed datasets still under their proprietary period are only accessible through ChaSeR.

NASA's HEASARC (High-Energy Astrophysics Science Archive Research Center) mirrors the CDA and provides several powerful interfaces (heasarc.gsfc.nasa.gov/docs/archive.html) to search and obtain publicly available datasets from for all currently operating X-ray missions and many past missions, where the observed data sets are recoverable, including both US and non-US missions. The Browse interface, in particular, is frequently used by the high-energy community. The TGCat (Transmission Grating Catalog, tgcate.mit.edu) includes all publicly available gratings observations processed through a pipeline developed by the HETG instrument team at MIT to provide calibrated gratings spectra and associated response files.

The *Chandra* Source Catalog (CSC, cxc.harvard.edu/csc) is the definitive catalog of X-ray sources detected by *Chandra*. By combining observations with similar pointings and taking advantage of the sub-arcsecond on-axis spatial resolution and using consistent data processing, the CSC provides a wide variety of uniformly calibrated properties and high level, science-ready data products for detected sources. The most comprehensive, interactive interface to explore the CSC and download data products is the CSCview application. The web-based Quick Search provides a limited, pre-defined

set of source properties and the sky coverage and source properties of the catalog can be explored and visualized using the CSC interface to the American Astronomical Society's World Wide Telescope (WWT), which provides the information to access the high level catalog data products and the individual observations in ChaSeR.

Ray Tracing/Simulations

A common use of the *Chandra* PSF is to simulate a challenging observation in order to demonstrate its feasibility for proposal planning; for example, resolving multiple or overlapping sources with unique spectra, HETG observations of extremely bright objects, or grating observations of extended sources. The most advanced method for characterizing the properties of the *Chandra* PSF is by simulating the PSF.

There are two parts to obtain a good model of the *Chandra* PSF. The first part is to simulate the PSF of the optics from the HRMA via photon ray tracing techniques and the second part is to project the simulated HRMA PSF onto the detector-plane. Instrumental effects may also be applied at the detector-plane which transforms the simulated photon rays into simulated X-ray events that make up a realization of the simulated *Chandra* PSF.

There are two primary means to simulate the HRMA PSF: SAOTrace and MARX (the Model of AXAF Response to X-rays).

SAOTrace

SAOTrace is a flexible system used to simulate the as-built X-ray optics with on-ground calibration by ray tracing; it is directly derived from the engineering tools used to design *Chandra*. While users can install SAOTrace on a local system for the greatest control and customization, the primary means most users will use SAOTrace is through the web-based interface *Chandra* Ray Tracer (ChaRT, cxc.cfa.harvard.edu/ciao/PSFs/chart2/). ChaRT is based on the most detailed physical model of the mirror geometry.

MARX

MARX is a suite of executables which allows users to readily run a large number of ray tracing simulations on a local system. While the MARX model uses a slightly simplified (and faster) description of the HRMA, this is often sufficient for most simulations.

MARX was created as a PSF simulator and not an observation simulator; therefore, not all CIAO tools are currently guaranteed to work on MARX simulated events files.

Whether the simulated rays are generated with SAOTrace/ChaRT or MARX, MARX will be used to project the simulated rays onto a detector-plane, since it provides the easiest interface to instrument models to estimate how the events would appear as observed. Within CIAO, there are wrapper scripts to simplify the use of MARX for projecting simulated ray files and running end-to-end simulations.

More Information

CXC science website
cxc.harvard.edu

Chandra Proposal Software (CPS)
cxc.harvard.edu/proposer/CPS.html

Proposers Observatory Guide (POG)
cxc.harvard.edu/proposer/POG/

Call for Proposals (CfP)
cxc.harvard.edu/proposer/CfP/

HelpDesk
cxc.harvard.edu/helpdesk/

CIAO
cxc.harvard.edu/ciao/

Proposer Information
cxc.harvard.edu/proposer/

Public Outreach site
chandra.harvard.edu/

What can Chandra do for you?

Science from recently accepted *Chandra* proposals

JWST Synergy

Use ultra-deep Chandra observations to study the X-ray emission from growing black holes in high-redshift JWST-identified galaxies.

Gravitational Waves

Identify, monitor, and characterize X-ray emission from compact-object mergers detected during upcoming LIGO/Virgo Observing Run.

Exoplanets

Measure the X-ray stellar irradiation (a major driver of photochemistry, upper atmospheric heating, and atmospheric mass loss) on habitable zone exoplanets by their M-star hosts.

Cosmology

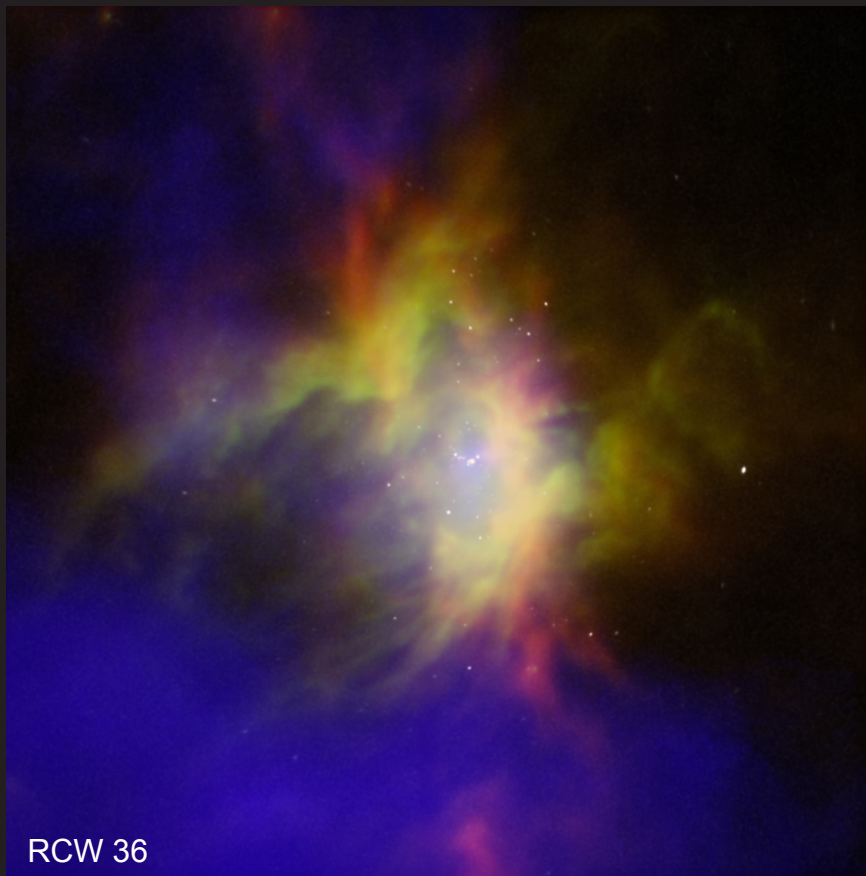
Probe X-ray absorption lines imprinted on the spectrum of background quasars to address the global and local missing baryon problems.

Archival Studies/Machine Learning

Use machine learning to identify high-energy transients in the complex, multi-parameter space of the Chandra Source Catalog 2.0.

Black Hole Simulations

Use constraints from Chandra observations to develop simulations of corona formation to help predict disk structure and dissipation as functions of accretion rate and disk magnetization.



RCW 36

*Credit: X-ray: NASA/CXC/Ames Research Center/L. Bonne et al.;
Infrared: ESA/NASA.JPL-Caltech/Herschel Space Observatory/JPL/IPAC*

Material preparation, layout, and editing by:

N.P. Lee and E.D. Tingle

Edition 1.0



**Don't need another handout to take home?
Want to help us save resources?**

Scan this code for the latest version of the *Chandra Pocket Guide*. We are always updating this document to better serve the next generation of X-ray astronomers.

Please send comments and new topic suggestions to cxchelp@cfa.harvard.edu.